Nonlinear Finite Element Solution of Post-buckling Responses of FGM Panel Structure under Elevated Thermal Load and TD and TID Properties

Subrata Kumar Panda[1,*], Trupti Ranjan Mahapatra[2], Vishesh Ranjan Kar[3]

[1]NIT, Rourkela: 769008, Odisha, India.
[2]KIIT University, Bhubaneswar: 751024, Odisha, India.
[3]VIT University, Vellore: 632014, Tamil Nadu, India.

*E-mail: call2subrat@gmail.com , pandask@nitrkl.ac.in

Abstract: - The nonlinear limited component answers for the buckling and post- buckling reactions of the functionally graded shell board subjected to the non-uniform thermal environment have been evaluated in this article. The thermal fields are expected as uniform, linear and nonlinear temperature ascend over the thickness of shell board and the properties of every constituent are thought to be temperature subordinate. The compelling material properties of the reviewed structure are assessed utilizing the Voigt's micromechanical rule in conjunction with power-law dissemination. For the examination reason, a general nonlinear numerical model of the functionally graded shell board has been produced based on the higher order shear deformation theory and Green-Lagrange sort geometrical nonlinear strains. The system governing equation of the board structure is inferred utilizing the variational rule. Further, appropriate nonlinear limited component steps have been received to discretize the model for the calculation of the desired responses in relationship with the direct iterative method. The convergence and the validation behavior of the present numerical model are at first tried to show its efficacy and significance. At last, the impacts of arch, power law index and different support conditions on the buckling and post- buckling reactions of the functionally graded shell boards are examined and talked about in subtle elements.

1. Introduction

The capacity of the functionally graded materials (FGMs) to withstand high thermal gradient have made them well known in many high performance engineering applications under outrageous temperature loading conditions. During service under sever thermal load, the FGM structures buckles and geometrical nonlinearity is instigated. The thought of the temperature dependent (TD) material properties (rather just considering temperature independent (TID) material properties alone) is especially basic for the correct investigation of their stability behaviour. The linear and nonlinear buckling and post- buckling conduct of FGM level/bended board subjected to uniform and non-uniform temperature stacking conditions was examined numerically by different scientists in past by utilizing the existing/refined shear deformation theories, for example, the Classical Plate Theory (CPT) [1-2], First Order Shear Deformation Theory (FOSDT) [3] and High Order Shear Deformation Theory (HOSDT) [5]. It is obvious from the survey of writing that, the FEM based numerical reviews identified with the geometrically nonlinear buckling and the post- buckling conduct of FG circular boards is extremely restricted [6-7]. Additionally, thinks about utilizing the CPT [8-9]/FOSDT [10-12] mid-plane kinematics are more in number in contrast with the HOSDT [13-15]. Analysts considered the through the thickness temperature variety to be uniform, linear and nonlinear and consolidated TD and TID material properties of the FG structures. Notwithstanding, in all the previously mentioned research to speak to the geometrical bending the von-Karman kind of nonlinear kinematics has been embraced as opposed to the Green-Lagrange sort that records for the disfigurement conduct of material continuum all the more precisely [16].

The inspiration of the present research is to concentrate the buckling and the post- buckling conduct of FG circular shell board by considering Green-Lagrange sort geometrical nonlinearity and the HOSDT mid-plane kinematics. In addition, the FG shell board properties are assessed utilizing Voigt's govern of blend in conjunction with the power-

law of circulation by taking both the TD and TID material properties. The representing condition of FG board is inferred utilizing the variational guideline and discretised utilizing a nine noded isoparametric Lagrangian component with nine degrees of freedom per node. A direct iterative strategy is utilized to acquire the desired responses.

2. Nonlinear Finite Element Formulations

Figure 1 demonstrates a common FG spherical shell board with a rectangular base with length 'a', width "b" and uniform thickness 'h', considered for the present examination. The curvature at the mid surface (at z = 0) of the shell board is characterized as 'R'. The relocation field in light of the HOSDT mid-plane kinematics as in [17]:

$$\left.\begin{aligned} u(x,y,z,t) &= u_0(x,y,t) + z\theta_x(x,y,t) + \\ &\quad z^2 u_0^*(x,y,t) + z^3\theta_x^*(x,y,t) \\ v(x,y,z,t) &= v_0(x,y,t) + z\theta_y(x,y,t) + \\ &\quad z^2 v_0^*(x,y,t) + z^3\theta_y^*(x,y,t) \\ w(x,y,z,t) &= w_0(x,y,t) \end{aligned}\right\} \quad (1)$$

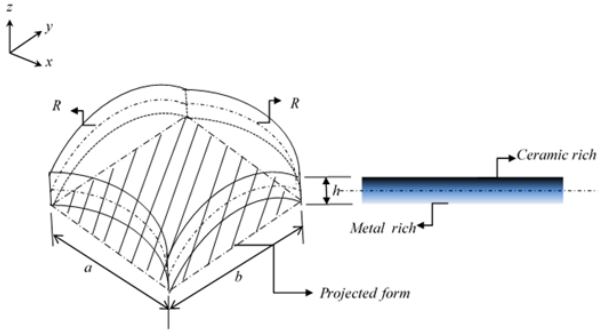

Figure 1. Geometry and dimension of FG spherical shell panel

where, (u0, v0, w0) speak to the comparing removals of the focuses on the mid-plane along (x, y, z) arranges, separately. θy and θx are the turns of ordinary to the mid-plane about the x and y hub, separately and are the higher request terms of the Taylor arrangement development characterized at the mid-plane those record for the allegorical circulation of shear stress.

The little strain and large deformation behavior of the FG shell board is communicated by considering Green-Lagrange sort nonlinear strain-dislodging field as in [18]

$$\{\varepsilon\} = \{\varepsilon_l\} + \{\varepsilon_{nl}\} \quad (2)$$

where, $\{\varepsilon_l\}$ and $\{\varepsilon_{nl}\}$ are the linear and the nonlinear strain tensors, respectively.

The temperature dependent material properties of the graded structure have been obtained using the equivalent steps as in the reference [19]. Now, the effective elastic and the thermal properties of the FGM are obtained via Voigt's micromechanics model using the following equation [15]:

$$P(T,z) = \{P_c(T,z) - P_m(T,z)\}\left(\frac{z}{h} + \frac{1}{2}\right)^n + P_m(T,z) \quad (3)$$

where, subscript '*m*' and '*c*' represent the ceramic and the metal constituents, respectively and P_0, P_{-1}, P_1, P_2 and P_3 are the coefficients of temperature (*T*) and *n* ($0 \le n < \infty$) is the power-law index.

The temperature function is expressed in the following form for uniform temperature variation:

$$T = T_m + \Delta T \text{ or } T = T_c \quad (4)$$

where, $\Delta T = T_c - T_m$ and T_m and T_c are the temperatures at the bottom and top surfaces of the panel, respectively. The detail of the linear temperature field through the thickness condition the temperature field is expressed as can be seen in Kar and Panda [16].

The thermo-elastic stress tensor at any point within the FG spherical shell panel can be written as

$$\{\sigma\} = \{\sigma_{xx} \quad \sigma_{yy} \quad \sigma_{xy} \quad \sigma_{xz} \quad \sigma_{yz}\}^T = [C](\{\varepsilon\} - \{\varepsilon_{th}\}) \quad (5)$$

where, $[Q]$ is the reduced stiffness matrix and $\{\varepsilon_{th}\} = \{1 \quad 1 \quad 0 \quad 0 \quad 0\}^T \alpha(T,z)\Delta T$ is the thermal strain tensor at any point within the shell panel and the details of $[C]$ can be seen in [16].

The elemental displacement vector is expressed using the corresponding shape function and the nodal displacement field as

$$\{\lambda_0\} = \sum_{i=1}^{9} N_i \{\lambda_{0_i}\} \tag{6}$$

where, $\{\lambda_{0_i}\} = \left[u_{0_i} \;\; v_{0_i} \;\; w_{0_i} \;\; \theta_{x_i} \;\; \theta_{y_i} \;\; u^*_{0_i} \;\; v^*_{0_i} \;\; \theta^*_{x_i} \;\; \theta^*_{y_i}\right]^T$ is the nodal displacement vector and N_i is the shape function for the i^{th} node, respectively. The details of the shape function can be seen in [19].

The linear and nonlinear mid-plane strain vector in terms of nodal displacement vector is written as

$$\{\bar{\varepsilon}_l\} = [B]\{\lambda_{0_i}\}, \quad \{\bar{\varepsilon}_{nl}\} = [A][G]\{\lambda_{0_i}\} \tag{7}$$

where, [*B*] and [*G*] are the product form of the differential operator matrix and the shape functions for the linear and the nonlinear strain vectors, respectively and [*A*] is the function of displacements associated with the nonlinear strain terms. For the details of [*B*], [*A*] and [*G*] matrices, [16] can be referred.

The strain energy expression can be conceded as:

$$U^e_\varepsilon = \frac{1}{2}\left(\{\lambda_{0_i}\}^T [K_l]^e \{\lambda_{0_i}\} + \{\lambda_{0_i}\}^T [K_{nl1}]^e \{\lambda_{0_i}\} + \{\lambda_{0_i}\}^T [K_{nl2}]^e \{\lambda_{0_i}\} + \{\lambda_{0_i}\}^T [K_{nl3}]^e \{\lambda_{0_i}\}\right) \tag{8}$$

The expressions for $[K_l]^e$, $[K_{nl1}]^e$ $[K_{nl2}]^e$ and $[K_{nl3}]^e$ can be seen in [18].

In the similar manner, the elemental equation of work done due to the in-plane thermal force resultant can be expressed as

$$W^e = \frac{1}{2}\{\lambda_{0_i}\}^T [K_G]^e \{\lambda_{0_i}\} \tag{9}$$

where, $[K_G]^e = \int_{-1}^{1}\int_{-1}^{1} [B_G]^T [D_G][B_G]|J| d\xi d\eta$ is the elemental geometric stiffness matrix.

The governing equation for the for the post-buckled FG spherical shell panel is obtained by minimizing the total energy expression. This result in

$$\delta(U^e_\varepsilon - W^e) = 0 \tag{10}$$

Now, substituting Eq. (8) and (9) into Eq. (10), the final form of the equilibrium equation for the post-buckled FG spherical shell panel is conceded to the following form:

$$\left(([K_l] + [K_{nl1}] + [K_{nl2}] + [K_{nl3}]) - \gamma_{cr}[K_G]\right)\{\Delta\} = 0 \tag{11}$$

where, γ_{cr} is the critical buckling load factor. [K_l], [K_{nl1}], [K_{nl2}], [K_{nl3}] and [K_G] are the corresponding global matrices of [K_l]^e, [K_{nl1}]^e, [K_{nl2}]^e, [K_{nl3}]^e and [K_G]^e, respectively.

3. Results and Discussion

With a specific end goal to figure the sought reactions, a custom made computer code has been created in MATLAB environment in light of the present nonlinear FE model of the FG board. The critical buckling and post-buckling reactions are processed by considering both the TD and TID material properties. For calculation, the silicon nitride (Si_3N_4) and the stainless steel (SUS304) are considered as the ceramic and the metal constituent at the top and at the base surface of the shell board, separately. The corresponding TD material properties are taken from the reference and subtle elements can be seen in [20].

Subsequent to setting up the convergence and validation of the present model the impacts of various support conditions, power-law index (*n*) and bend proportion (*R*/*a*) on the post-buckling reactions of FG round board under various temperature fields have been examined. The relating reactions for FG level board are additionally exhibited for examination. The different support conditions utilized for the present examination can be seen in [16]:

3.1 Convergence and Validation Study

Initial, a merging review has been performed to take note of the exact mesh size at which the present model is equipped for figuring the linear and nonlinear post-buckling reactions for the FG shell board. The wanted reactions are registered for FG spherical (*R*/*a*=5, *n*=2, *a*/*h*=10) board with SSSS support condition and level (*n*=0.2 and 5, *a*/*h*=10) board with CSCS support condition and displayed in Figure 2 (*a*) and (*b*), separately. The reactions are acquired for various work sizes and abundancy proportions (W_{max}/*h*=0, 0.5, 1 and 1.5) by considering different through the thickness temperature distribution (uniform, linear and nonlinear). It is obviously watched that the

reactions are merging admirably with work refinement for both the round and level boards. In light of the convergence study a (5×5) mesh is utilized to figure the thermal post-buckling reactions all through the present review.

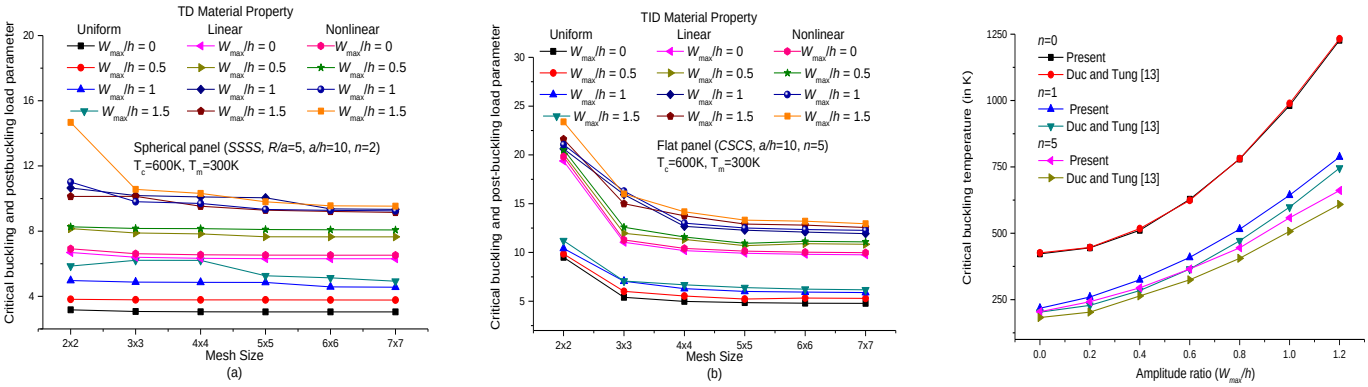

Figure 2. Convergence behavior of the thermal buckling and post-buckling responses of (*a*) TD-FG spherical panel and (*b*) TID-FG flat panel

Figure 3. Comparison of the thermal post-buckling responses of simply supported FG (Al/Al_2O_3) flat panel.

At that point the approval of the present model is offered by considering a FG (Al/Al_2O_3) flat (a/h=20 and a/b=1) board, as the flat boards are thought to be the least difficult type of the shell board. The thermal post-buckling reactions are processed under the uniform temperature ascend for three different power-law indices (n = 0, 1 and 5) and exhibited in Figure 3 together with the accessible aftereffects of Duc and Tung [13]. The material and geometrical parameters are taken to be the same as in the reference [13]. It is watched that the present outcomes are showing higher basic buckling temperature values when contrasted with Duc and Tung [13]. It is on the grounds that, the present model records the full geometrical nonlinearity in Green-Lagrange sense though, in the reference, the nonlinearity is presented by means of von-Karman strain which is unrealistic to consider the correct geometrical twisting under the severe thermal load.

3.2 Additional Illustrations

In this area, some more numerical outlines are exhibited to demonstrate the relevance of the present created model to register the post-buckling conduct of FG ($SUS304/Si_3N_4$) circular shell board under shifting thermal loading conditions. The temperatures at the base and the highest point of the shell board are thought to be Tm=300K and Tc=600K, respectively and both the TD and TID material properties are considered for calculation of the reactions. To perform a comparative examination, the reactions are additionally processed for level board (R=∞) under indistinguishable geometry, material properties and constraint conditions.

Table 1. Effect of support conditions on the critical buckling and post-buckling responses (γ_{cr}) of the FG spherical and flat panel

Temperature field	TD/ TID	Support conditions	Flat Panel W_{max}/h				Spherical (R/a=10) W_{max}/h			
			0	0.5	1	1.5	0	0.5	1	1.5
Uniform	TID	SSSS	3.096	3.333	4.054	5.223	3.179	3.699	4.634	4.921
		SCSC	5.247	5.664	6.612	6.890	5.328	6.335	6.627	6.983
	TD	SSSS	2.728	2.942	3.565	3.788	2.807	3.283	4.150	4.471
		SCSC	4.914	5.499	7.027	7.126	5.004	6.037	7.558	7.256
Linear	TID	SSSS	6.420	6.971	8.569	8.908	6.581	7.524	9.640	10.154
		SCSC	10.903	12.148	13.493	14.373	11.051	13.172	13.703	14.792
	TD	SSSS	5.727	6.058	7.613	8.883	5.870	6.869	8.776	9.065
		SCSC	9.721	10.832	12.027	12.701	9.852	11.738	12.283	12.855
Non Linear	TID	SSSS	6.628	7.175	8.749	29.375	6.793	7.948	10.130	10.431
		SCSC	11.254	12.541	13.963	14.714	11.406	13.548	14.234	15.001
	TD	SSSS	5.923	6.417	7.866	8.224	6.070	7.115	8.275	9.364
		SCSC	10.054	11.202	14.139	13.135	10.188	12.124	12.703	13.394

*3.2.1 Influence of temperature field*The impact of various temperature fields to be specific uniform, linear and nonlinear temperature circulation through the thickness on the buckling and the post-buckling reactions of the square (a/b=1) FG (SUS304/Si_3N_4) spherical (R/a=10) and level board (a/h=10, n=2) has been inspected in this case. The responses are computed for various support conditions (SSSS and CSCS) and introduced in Table 1. It is watched that the basic buckling and post-buckling load parameters are most astounding for the nonlinear temperature distribution and least for all uniform condition. The post-buckling reactions are higher for round board than the level ones. Be that as it may, the FG spherical board with the TD properties is demonstrating the sub-par buckling and the post-buckling quality in contrast with the FG spherical board with TID properties.

3.2.2 Influence of power-law index: In this case, the impact of power-law index on the clasping and the post-buckling reactions of simply supported thick (a/h=10) square FG (SUS304/Si_3N_4) spherical (R/a=5) and flat panel with TD and TID properties has been explored and introduced in Figure 4 (*a*)-(*c*), respectively. It is noticed that, as the FGM gets to be distinctly metal rich, the post-clasping reactions for both round and level board are decreasing monotonously. This is normal as the ceramic has relatively higher stiffness than the metal. Additionally, the FG level and round board indicate most astounding buckling and the post-buckling quality under the nonlinear temperature field in comparison with the other temperature fields.

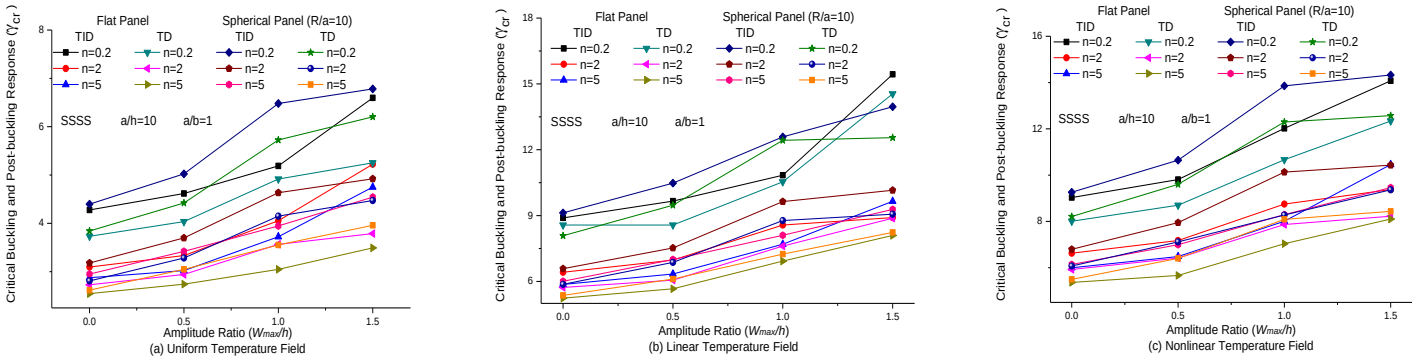

Figure 4. Effect of power-law indices on the critical buckling and post-buckling responses (γ_{cr}) of FG spherical (R/a=10) and flat panel under (a) Uniform (b) Linear and (c) Nonlinear temperature field.

3.2.5 Effect of curvature ratio: It is inferred from the previous examples that the spherical panels exhibit higher buckling and post-buckling strength over the flat panel due to their spatial curvature. Therefore, the buckling and the post-buckling responses (γ_{cr}) of the thin (a/h=50) shallow FG spherical shell panel (a/b=1, n=2 and CSCS) under the effect of various curvature ratios (R/a=10, 50, 100) have been investigated in this example. The post-buckling responses are computed for uniform, linear and nonlinear temperature fields and presented in Figure 5 (a)-(c), respectively. It is observed that the buckling and the post-buckling load parameters are decreasing as the panel tend to become flat.

4. Conclusion

In this article, the buckling and post-buckling quality of FGM structure have been examined utilizing another new higher-order model under raised thermal documented and distinctive geometrical designs. The effective material properties of the FGM are assessed by means of the Voigt's micromechanical show in conjunction with the power-law distribution. Moreover, both the TD and TID material properties of the FG board are considered in the present investigation. It is seen from the present outcomes that the TD material properties and the Green-Lagrange sort geometrical nonlinearity in conjunction with the HOSDT model for the thermal stability of the FG board structures are inevitable. It is inferred that as the power-law index increment the instability of the FGM board is upgraded.

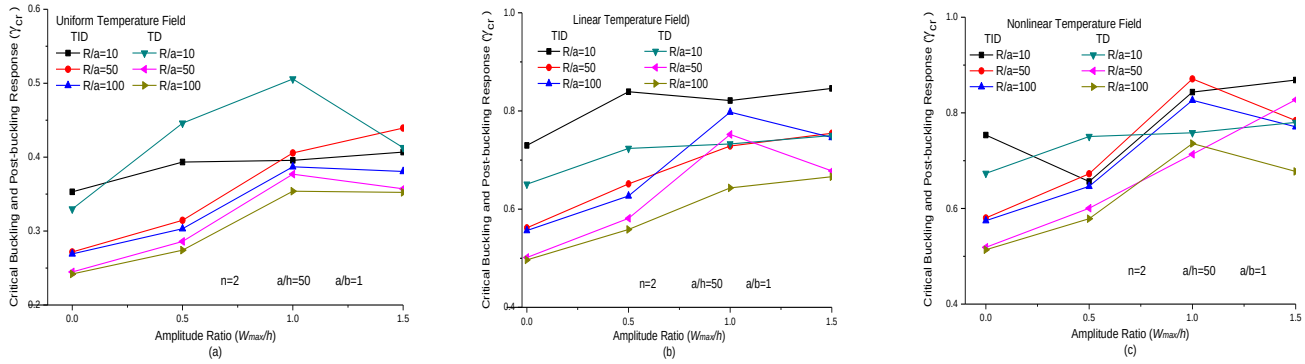

Figure 5. Effect of curvature ratio on the critical buckling and post-buckling responses (γ_{cr}) of FG spherical panel under (a) Uniform (b) Linear and (c) Nonlinear temperature field.

References

[1] Ghannadpour S A M, Ovesy H R and Nassirnia M 2012 *Computers and Structures* **108(109)** 93–99.
[2] Huang H, Han Q, Feng N and Fan X 2011 *Mechanics of Advanced Materials and Structures* **18(5)** 337–46.
[3] Zhao X, Lee Y Y and Liew K M 2009 *Composite Structures* **90(2)** 161–171.
[4] Shen H S, 2007 *International Journal of Mechanical Sciences* **49(4)** 466–478.
[5] Thai H and Kim S 2015 *Composite Structures* **128** 70-86.
[6] Na K S and Kim J H 2004 *Composites Part B Engineering* **35(5)** 429–437.
[7] Duc N D and Quan T Q 2012 *Mechanics of Composite Materials* **48(4)** 435-448.
[8] Shen H S 2004 *International Journal of Solids Structures* **41(7)** 1961–1974.
[9] Wu T L, Shukla K K and Huang J H 2007 *Composite Structures* **81(1)** 1–10.
[10] Park J S and Kim J H, 2006 *Journal of Sound and Vibration* **289(1-2)** 77–93.
[11] Prakash T, Singha M K and Ganapathi M 2008 *Engineering Structures* **30(1)** 22–32.
[12] Liew K M, Yang J and Kitipornchai S 2004 *Journal of Applied Mechanics* **71(6)** 839–850.
[13] Duc N D, Tung H V 2011 *Composite Structures* **93(11)** 2874–2881.
[14] Shen H S and Wang H 2014 *Aerospace Science and Technology* **38** 9-19.
[15] Kar V R and Panda S K 2015 *Composite Structures* **129** 202–212.
[16] Reddy J N and Chin C. D. 1998 *Journal of Thermal Stresses* **21** 593–626.
[17] Reddy J N 2004 *Mechanics of laminated Composite Plates and Shells* Second Edition CRC Press.
[18] Cook R D, Malkus D S, Plesha M E and Witt R J 2009 *Concepts and applications of finite element analysis* Fourth Edition John Willy and Sons (Asia) Pvt. Ltd., Singapore.
[19] Huang X L and Shen H S, 2004 *International Journal of Solids Structures* **41(9-10)** 2403–2427.